Bioorganic & Medicinal Chemistry Letters 22 (2012) 2283–2286

Contents lists available at SciVerse ScienceDirect

Bioorganic & Medicinal Chemistry Letters

journal homepage: www.elsevier.com/locate/bmcl

Design and evaluation of a series of pyrazolopyrimidines as p70S6K inhibitors

Joerg Bussenius *, Neel K. Anand, Charles M. Blazey, Owen J. Bowles, Lynne Canne Bannen, Diva S.-M. Chan, Baili Chen, Erick W. Co, Simona Costanzo, Steven C. DeFina, Larisa Dubenko, Stefan Engst, Maurizio Franzini, Ping Huang, Vasu Jammalamadaka, Richard G. Khoury, Moon H. Kim, Rhett R. Klein, Douglas Laird, Donna T. Le, Morrison B. Mac, David J. Matthews, David Markby, Nicole Miller, John M. Nuss, Jason J. Parks, Tsze H. Tsang, Amy L. Tsuhako, Yong Wang, Wei Xu, Kenneth D. Rice

Exelixis, 210 E. Grand Avenue, South San Francisco, CA 94080, USA

ARTICLE INFO

Article history:
Received 20 December 2011
Revised 17 January 2012
Accepted 20 January 2012
Available online 2 February 2012

Keywords:
p70S6K inhibitor
Pyrazolopyrimidine
PI3K pathway
Cancer

ABSTRACT

The 70-kDa ribosomal protein S6 kinase (p70S6K) is part of the PI3K/AKT/mTOR pathway and has been implicated in cancer. High throughput screening versus p70S6K led to the identification of aminopyrimidine **3a** as active inhibitor. Lead optimization of **3a** resulted in highly potent, selective, and orally bioavailable pyrazolopyrimidines. In this manuscript we report the structure–activity relationship of this series and pharmacokinetic, pharmacodynamic, and efficacy data of the lead compound **13c**.

Hyperactivated signaling due to dysregulation of the phosphoinositide 3-kinase (PI3K)/phosphatase and tensin homolog on chromosome ten (PTEN) pathway is observed in many cancers and correlates with tumor growth and survival.[1] These observations suggest that inhibitors targeting components of the PI3K/PTEN kinase cascade may have utility for therapeutic intervention in cancer, and several excellent reviews describing this strategy have been published.[2–5] The last kinase of the PI3K/AKT/mammalian target of rapamycin (mTOR) pathway is the 70-kDa ribosomal protein S6 kinase (p70S6K). p70S6K is a serine/threonine kinase that belongs to the AGC kinase family.[6] In response to activation by a complex of mTOR with two proteins, Raptor and GβL (this complex is commonly referred to as TORC1), p70S6K phosphorylates the S6 protein of the 40S ribosomal subunit. Phosphorylation of S6 is involved in translational control of 5′ oligopyrimidine tract mRNAs and ultimately results in upregulation of cellular protein synthesis.[7]

As part of our overall strategy to develop kinase inhibitors with different inhibition profiles within the PI3K/Akt/mTOR pathway we were interested in investigating the selective inhibition of p70S6K, which has been targeted by other groups as well.[8]

Our p70S6K research program began with a high throughput screening campaign of our internal small molecule library against p70S6K. This campaign led to the identification of the 4-amino-5-nitropyrimidine-containing inhibitor **3a** with an IC_{50} of 85 nM (no activity below 2000 nM against any other kinase of our in-house panel), which was considered acceptable for further structure–activity optimization efforts (Table 1).[9] These efforts consisted of two separate activities which were carried out in parallel. First, to improve the biochemical activity of **3a**

Table 1
Biochemical activity of compounds **3a–h**

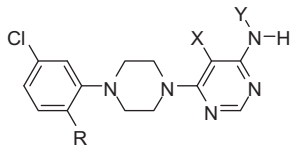

ID	X	Y	R	p70S6K IC_{50} (nM)
3a	NO_2	H	H	85
3b	NO_2	H	Me	3
3c	H	H	H	>2000
3d	Me	H	H	>2000
3e	N = CH		H	196
3f	CH = CH		H	162
3g	CH = N		H	107
3h	CH = N		Me	13

* Corresponding author. Tel.: +1 6508377000; fax: +1 6508378177.
E-mail address: jbusseni@exelixis.com (J. Bussenius).

0960-894X/$ - see front matter © 2012 Elsevier Ltd. All rights reserved.
doi:10.1016/j.bmcl.2012.01.105

we embarked on a survey of different substitution patterns on the phenylpiperazine part of the molecule. A total of 55 compounds were evaluated, and from this set the 2-methyl-5-chlorophenylpiperazine **3b** had the lowest IC_{50} of 3 nM (Table 1). Second, we were concerned about the potential for multistep reductive bioactivation forming hazardous metabolites from the nitro group contained in **3a**[10] and therefore directed our efforts to find a replacement for this substituent. Complete removal (compound **3c**) or substitution with other small groups (e.g., **3d**) resulted in significant loss of activity. More successful was the incorporation of both the nitro and the amino nitrogens in an imidazole heterocycle. The resulting imidazopyrimidine **3e** exhibited only a twofold loss of activity compared to **3a**. Encouraged by this result we also prepared the pyrrolopyrimidine **3f** and pyrazolopyrimidine **3g**. In particular the pyrazolopyrimidine **3g** was almost as active as the original HTS hit **3a**. We then synthesized compound **3h** to determine if the SAR from the phenylpiperazine pattern translated from the nitropyrimidines to the new pyrazolopyrimidine. Indeed, by making the small change from **3g** to **3h** the biochemical activity was increased almost tenfold. Compound **3h** was viewed as lead compound for further SAR development, considering the improvement of biochemical activity and reduction of potential metabolic liabilities over HTS hit **3a**. The compounds in Table 1 were prepared by reaction of commercially available chloropyrimidine analogs or the corresponding bicyclic systems with either 3-chlorophenylpiperazine or 5-chloro-2-methylphenylpiperazine as illustrated in Scheme 1.

Despite good biochemical activity, compound **3h** only had an IC_{50} of 1.1 μM in the cellular S6 phosphorylation assay in A549 cells (Table 2).[11] We therefore planned on increasing the lipophilicity of the compounds to improve permeability. To get a better understanding of which modifications could be beneficial, homology models of p70S6K were constructed based on the crystal structure of active (PDB code 1O6L) and inactive (PDB code 1GZK) Akt (PKB). The model proposed binding of the pyrazole NH with the carbonyl of Glu173 and the pyrimidine N-7 with the backbone NH of Leu175 in the kinase hinge region. The model also predicted that substitution in the 6-position of the pyrazolopyrimidine would not be tolerated, since it was too close to the C=O of the backbone of Leu175. This was confirmed experimentally by compound **4** (Table 2). On the other side, substitution on C-3 with a hydrophobic group seemed to be favorable. The synthesis of compounds **5a** and **5b** with increased steric bulk in the 3-position suggested that this proposal was also correct. In addition to a positive effect on biochemical activity, the structural change resulted in compounds with increased lipophilicity as indicated by their

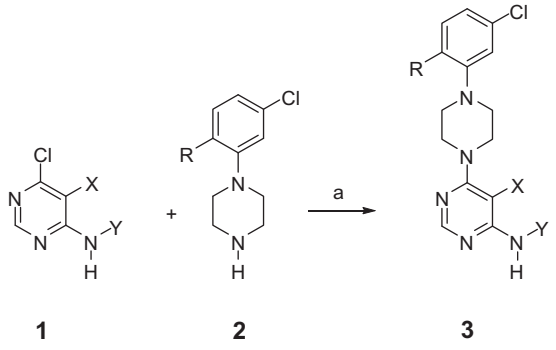

Scheme 1. Synthesis of compounds **3** (for detailed structures see Table 1). Reagents and conditions: (a) EtOH, DIEA, 70 °C, 4–15 h, (for **3c**: NMP, DIEA, 180 °C, 16 h; for **3d**: DMSO, DIEA, 140 °C, 15 h).

Table 2
Activity of substituted pyrazolopyrimidines

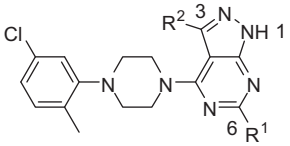

ID	R^1	R^2	p70S6K IC_{50} (nM)	A549 Cell IC_{50} (nM)	*c*log*P*
4	Me	H	>2000	–	4.0
3h	H	H	13	1132	3.5
5a	H	Me	9	500	3.8
5b	H	Et	6	150	4.3
5c	H	iPr	16	207	4.7
5d	H	nPr	6	275	4.9
5e	H	Br	7	86	4.4
5f	H	CF_3	29	41	4.5

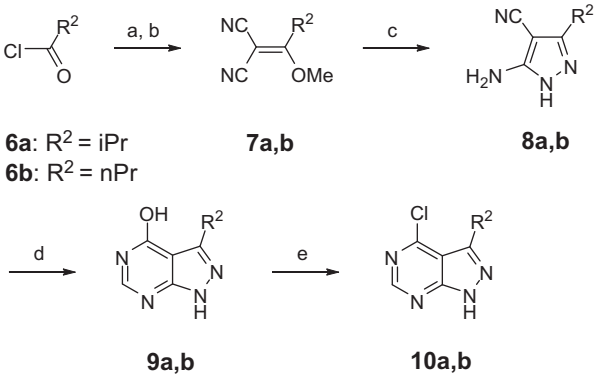

Scheme 2. Synthesis of non-commercial chloropyrazolopyrimidines. Reagents and conditions: (a) malononitrile, THF, NaH, rt, 16; (b) TMS-diazomethane, Et_2O, MeOH, 0 °C, 3 h; (c) hydrazine monohydrate, EtOH, 80 °C, 3 h; (d) formic acid, 110 °C, 4 h; (e) $SOCl_2$, DMF, reflux, 2 h.

Table 3
Activity of solubilized analogs

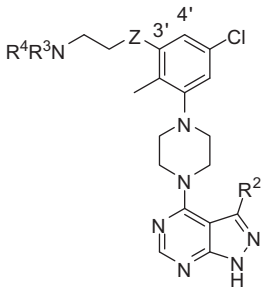

ID	R^2	Z	NR^3R^4	p70S6K IC_{50} (nM)	A549 Cell IC_{50} (nM)
11a	Et	O	NEt_2	11	339
12a	Et	CH_2	NEt_2	3	211
13a	Et	NH	NEt_2	3	184
11b	Et	O		5	243
12b	Et	CH_2		2	152
13b	Et	NH		3	80
11c	Et	O	NMe_2	6	143
13c	Et	NH	NMe_2	2	45
14	Br	NH	NMe_2	2	43
15	CF_3	NH	NMe_2	4	50

*c*log*P* values, and also significantly increased their cellular potencies (Table 2). However, there are limitations to the overall size of this group. Larger alkyl substituents as in **5c** or **5d** showed no benefit in biochemical activity and also led to a reduction in cell based potency. The SAR motivated us to focus on the improved lead compound **5b** for ongoing optimization. Also of interest were the bromo-compound **5e** and the trifluoromethyl analog **5f**, since both substituents resulted in further improvements in cellular potency.

For the synthesis of the compounds shown in Table 2 the same reaction as described in Scheme 1 was used. The required substituted 4-chloropyrazolopyrimidines were either commercially available (R^2 = H, Me, Et, Br, CF_3); or prepared according to Scheme 2 (R^2 = iPr, nPr). Condensation of malononitrile with either butyryl- or isobutyryl chloride afforded enols, which were treated with TMS-diazomethane to give the enolethers **7a,b**. Cyclization of **7a,b** with hydrazine provided the pyrazoles **8a,b**. Compounds **8a,b** were then transformed into the chloropyrazolopyrimidines **10a,b** by condensation with formic acid followed by chlorination with thionyl chloride.

With compound **5b** being very active in the biochemical assay and also showing good potency in the cell, we were interested in its pharmacokinetic profile, which was determined in the rat. As shown in Table 4, the compound exhibited poor oral absorption and low oral bioavailability. To overcome these liabilities we chose to incorporate a basic amino group in order to improve aqueous solubility. Our homology model predicted substitution at C-3′ on the phenyl group as most likely to avoid negative interactions with the protein. The 4′-position on the other hand was too close to the G-loop of the enzyme to allow appropriate substitution. Evaluation of compounds with basic amino groups attached via oxygen, carbon, and nitrogen on C-3′ of the phenyl moiety (**11a–c, 12a** and **b, 13a–c**, Table 3) indeed showed good tolerance for these substituents. While all the compounds are very potent, two trends can be observed. First, the biochemical activities of the C and N linked compounds are comparable, and both are considerable higher than the O analogs. For the O analogs the reduced biochemical activity is also reflected in lower cellular potency. Second, despite almost identical biochemical activities of the C and N analogs, the N linked compounds show significantly higher cellular potency. In particular the dimethyl-aminoethyl-amino analog **13c** demonstrates excellent potency against S6 phosphorylation in A549 cells. Replacement of the ethyl group on the pyrazolopyrimidine with a bromo- (**14**) or trifluoromethyl-substituent (**15**) did not result in any improvement of cell based activity over **13c** in contrast to our observations of the unsolubilized analogs **5b**, **5e**, and **5f**.

Ethyl analog **13c** also had the best selectivity profile compared to **14** or **15**. When screened against our in-house kinase panel, compound **13c** showed no cross reactivity towards non-AGC kinases (IC_{50} >1000 nM). However, some activity towards AGC

Table 4
Comparison of rat PK properties of compound **5b** with **13c**

ID	Dose (mg/kg)	CL (mL/h/kg)	V_d (L/kg)	$T_{1/2}$ (h) IV/PO	*F* (%)	C_{max} (μM) IV/PO	AUC/dose (μM h kg/mg) IV/PO
5b	2.5	1549	6.3	7.1/1.4	2	6.29/0.03	1.74/0.02
13c	2.5	1044	3.7	2.9/3.3	23	1.47/0.15	1.72/0.45

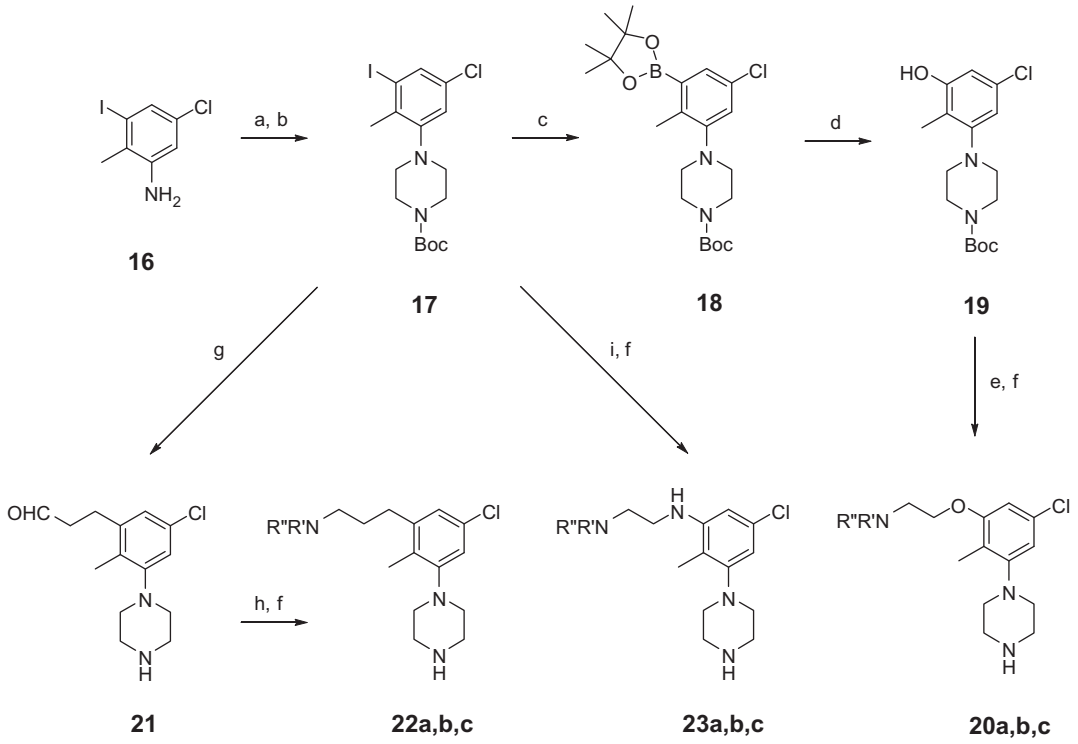

Scheme 3. Preparation of phenylpiperazines used for products listed in Table 3. Reagents and conditions: (a) bis(2-chloroethyl)amine, diglyme, K_2CO_3, reflux, 24 h, 40%; (b) di-*tert*-butyldicarbonate, THF, rt, 15 h, 92%; (c) bis(pinacolato)diborane, $PdCl_2$dppf, KOAc, DMSO, 80 °C, 24 h, 48%; (d) H_2O_2, NaOH, THF, rt, 30 min, quantitative; (e) substituted chloroethylamine (**a**: NR′R″ = NEt_2, **b**: NR′R″ = pyrrolidine, **c**: NR′R″ = NMe_2), Cs_2CO_3, DMF, rt, 16 h; (f) HCl, dioxane, MeOH, reflux, 2 min; (g) allyl alcohol, $NaHCO_3$, $Pd(OAc)_2$, TBAC, DMF, 50 °C, 4 h, 69%; (h) amine (**a**: diethylamine, **b**: pyrrolidine, **c**: dimethylamine), $NaB(OAc)_3H$, dichloroethane; (i) corresponding aminoethylamine, NaOtBu, XANTPHOS, $Pd_2(dba)_3$, dioxane, reflux, 5 h.

kinases, particularly Rsk2 (68 nM) and PKA (42 nM) were observed. For the two Akt isoforms Akt1 and Akt2 only weak activity was measured (371 and 3021 nM, respectively). Compound **14** on the other hand had stronger activity against AGC kinases (Akt1: 53 nM, Akt2: 311 nM, Rsk2: 248 nM, and PKA: 25 nM). Additionally, this compound showed some cross reactivity with IC_{50}s <500 nM against several other targets outside the AGC kinase family (e.g., PIM1). Further, the trifluoromethyl-analog **15** was also active against AGC kinases (Akt1: 74 nM, Akt2: 477 nM, Rsk2: 24 nM, and particularly PKA with 6 nM).

On the basis of these in vitro data we decided to take compound **13c** forward into in vivo studies. First, the pharmacokinetic profile of **13c** was determined in the rat and the results are summarized in Table 4. Compared to compound **5b**, the absorption and oral bioavailability were significantly improved. This result in combination with the high potency led to the advancement of **13c** into a mouse pharmacodynamic study in which the inhibition of S6 phosphorylation was measured. In this study **13c** demonstrated >60% inhibition at 100 mg/kg PO dosing in the PC3 prostate carcinoma model. Compound **13c** was subsequently evaluated in a PC3 xenograft efficacy experiment and dosed orally at 30, 100, and 300 mg/kg twice a day for 14 days. The compound was also active in this study and showed a good dose–response relationship with 21%, 49%, and 69% tumor growth inhibition, respectively

Scheme 3 describes the synthesis of highly functionalized phenylpiperazines needed for the preparation of the products shown in Table 3. Reaction of aniline **16** with bis(2-chloroethyl)amine followed by protection with di-*tert*-butyl dicarbonate yielded iodophenylpiperazine **17**. Palladium mediated conversion of **17** into pinacolester **18** and oxidation with hydrogen peroxide gave phenol **19**, which was then alkylated with chloroethylamines followed by deprotection to afford the phenylpiperazines **20a–c**, where the basic amino group is attached to the phenyl ring via oxygen. The preparation of the corresponding compounds **22a–c**, in which the basic amine was tethered to the phenyl ring through a propyl linker, was carried out by Heck reaction of iodophenylpiperazine **17** with allyl alcohol,[12] followed by reductive amination and deprotection. Finally, the nitrogen linked analogs **23a–c** were synthesized by Buchwald–Hartwig amination of **17** followed by deprotection of the Boc group. The coupling of these phenylpiperazines with the respective chloropyrazolopyrimidines was then carried out again as described in Scheme 1.

In summary, we have outlined the successful optimization of novel and highly potent p70S6K inhibitors based on the pyrazolopyrimidine structural motif. The resulting lead compound **13c** is selective over other kinases, has a reasonable ADME profile, and is efficacious in the PC3 xenograft model. Further optimization of **13c** leading to clinical candidate XL418 will be reported in due course.

Acknowledgments

The authors appreciate the contributions of the following persons. Steven Richards for help with the manuscript. Tracy Lou for conducting the biochemical assays and Edith Ubannwa for executing cell based assays. Julie Ren and Yeping Zhao generated the PK data. Paul Keast, Wendy Abulafia, Brian Sutton, and Teresa Carabeo performed the PD experiment and Jason Chen and F. Michael Yakes the efficacy study.

References and notes

1. Vivanco, I.; Sawyers, C. L. *Nat. Rev. Cancer* **2002**, *2*, 489.
2. Hennessy, B. T.; Smith, D. L.; Ram, P. T.; Lu, Y.; Mills, G. B. *Nat. Rev. Drug Discovery* **2005**, *4*, 988.
3. Engelman, J. A. *Nat. Rev. Cancer* **2009**, *9*, 550.
4. Liu, P.; Cheng, H.; Roberts, T. M.; Zhao, J. J. *Nat. Rev. Drug Discovery* **2009**, *8*, 627.
5. Courtney, K. D.; Corcoran, R. B.; Engelman, J. A. *J. Clin. Oncol.* **2010**, *28*, 1075.
6. Matthews, D. J.; Gerritsen, M. E. *Targeting Protein Kinases for Cancer Therapy*; John Wiley & Sons: Hoboken, NJ, 2010. 274–275 and 282–283.
7. Thomas, G. *Biol. Res.* **2002**, *35*, 305.
8. (a) Bandarage, U.; Hare, B.; Parsons, J.; Pham, L.; Marhefka, C.; Bemis, G.; Tang, Q.; Moody, C. S.; Rodems, S.; Shah, S.; Adams, C.; Bravo, E.; Savic, V.; Come, J. H.; Green, J. *Bioorg. Med. Chem. Lett.* **2009**, *19*, 5191; (b) Ye, P.; Kuhn, C.; Juan, M.; Sharma, R.; Connolly, B.; Alton, G.; Liu, H.; Stanton, R.; Kablaoui, N. M. *Bioorg. Med. Chem. Lett.* **2011**, *21*, 849.
9. p70S6K assay: kinase activity was measured as the percent of ATP consumed following the kinase reaction using luciferase–luciferin-coupled chemiluminescence. Reactions were conducted in 384-well white, medium binding microtiter plates (Greiner). P70S6 Kinase reactions were initiated by combining test compounds, 500 nM ATP, 3 μM RRRLSSLRA (Synpep), and 12 nM Human p70S6K (residues 1–421, contains D18H and T412E mutations, Upstate Bio-technology) in 20 μL of reaction buffer (20 mM Hepes pH 7.5, 10 mM $MgCl_2$, 0.03% NP40, 0.03% BSA, 1 mM DTT). The reaction mixture was incubated at ambient temperature for 3 h after which 20 μL aliquot of luciferase–luciferin mix (50 mM HEPES, pH 7.8, 67 mM oxalic acid (pH 7.8), 5 (or 50) mM DTT, 0.4% Triton X-100, 0.25 mg/mL coenzyme A, 63 mM AMP, 28 mg/mL luciferin and 40,000 units/mL luciferase) was added and the chemiluminescence signal measured using a Victor2 plate reader (Perkin–Elmer).
10. Boelsterli, U. A.; Ho, H. K.; Zhou, S.; Leow, K. Y. *Curr. Drug Meta.* **2006**, *7*, 715.
11. A549 cell assay: cells were seeded in 96-well plates (all plates and dishes are NUNC unless otherwise noted) in DMEM (Cellgro) containing 10% FBS (all FBS is heat-inactivated and from Hyclone unless otherwise noted), 1% penicillin–streptomycin (Cellgro), and 1% non-essential amino acids (Cellgro). A549 cells were seeded at 7.5 × 103cells/well. Cells were incubated at 37 °C, 5% CO_2 for 48 h. Test compound in DMSO was diluted in DMEM. The DMSO concentration in cell culture medium was maintained at 0.2% in all wells. Cells were treated with diluted compound and each concentration assayed in triplicate at concentrations of 1.2–300 nM, 0.004–1 nM rapamycin (Cell Signaling Technology, 9904) and 0.12–30 nM staurosporine (Calbiochem, 569396) served as positive controls. Negative control wells were treated with DMSO. Cells were incubated for 3 h at 37 °C, 5% CO_2 for 3 h in the presence of compound. Post compound treatment cells were fixed as follows: medium was removed and 100 μl/well of 4% formaldehyde (Sigma–Aldrich, 08920AD) in TBS (Pierce, 28376) was added to each well at room temperature (rt) for 20 min. Cells were quenched with 100 μl 0.6% H_2O_2 (VWR International, 43038308) in TBS (Pierce, 28376) +0.1%Tween20 (Sigma, P-7949) (TBST) for 20 min at rt. Plates were washed 3× with 200 μl TBS and blocked with 100 μl 5% BSA (Jackson ImmunoResearch Laboratory, 001-000-162) in TBST for 1 h at rt. Anti-phospho-S6 ribosomal protein antibody (Cell Signaling Technology, Ser 240/244 2212L) and anti-total-S6 ribosomal protein antibody (Cell Signaling Technology, 2215L) were diluted 1:200 in 5% BSA in TBST. Fifty microlitre primary antibody solution was added to each well and incubated overnight at 4 °C. Plates were washed 3× with 200 μl TBST. Goat anti-rabbit secondary antibody (Chemicon International, 24070101) was diluted at 1:20000 in 5% non-fat dry milk in TBST. 50 μl of antibody solution was added to each well and incubated for 1 h at rt. Plates were washed 3× with 200 μl TBST and 2 × 200 μl TBS. Chemiluminescent substrate (Super Signal Elisa Femto Chemiluminescent Substrate; Pierce, 37075) was prepared at rt. Hundred microlitre of chemiluminescent substrate per well was added and then the plate was shaken for 1 min. Luminescence was read immediately on a Wallac plate reader.
12. Melpolder, J. B.; Heck, R. F. *J. Org. Chem.* **1976**, *41*, 265.